Available online at www.sciencedirect.com

SCIENCE DIRECT®

Journal of Nuclear Materials 335 (2004) 199–203

journal of nuclear materials

www.elsevier.com/locate/jnucmat

# Mass transfer of iron impurities in LBE loops under non-isothermal flow conditions

T. Malkow, H. Steiner, H. Muscher *, J. Konys

*Forschungszentrum Karlsruhe GmbH, Institut für Materialforschung III, 76021 Karlsruhe, Germany*

---

## Abstract

Lead–bismuth eutectic (LBE) regained interest as a target and a nuclear coolant in nuclear applications. However, the corrosion of the structural materials such as ferritic/martensitic and austenitic stainless steels remains a major issue. Usually, their corrosion behavior measured as the mass transfer by dissolution/precipitation of metal solutes in non-isothermal flowing LBE is tested in loop systems. The exposures usually last for several thousand hours but, to date, almost no reliable long-term experience is reported. A mass transfer model based on species conversion and experimentally verified flow parameters is proposed and applied to predict the corrosion rate of iron solute at dissolved oxygen levels typical for active oxygen control in LBE. The sensitivity of the model indicates that iron diffusion seems to play a decisive role.

---

## 1. Introduction

Recently, LBE gained renewed interest in nuclear applications such as accelerator driven systems (ADS) [1–6]. The corrosion of the structural materials mainly steels is a great concern particularly the dissolution of their base and alloying elements [4,7–10] leading to coolant contamination but more deleterious to the structural integrity. Component clogging and plugging may occur as a result of solute precipitation likely in a non-isothermal regime. Long-term corrosion data acquired in loop tests [8,10–15] are an absolute necessity for real ADS but are so far scarce. Modeling seems thus an attractive option. Here, a mass transfer model is derived to predict exemplarily the corrosion (dissolution/precipitation) rate of iron stemming from a stainless steel exposed to non-isothermal LBE flowing in the CORRIDA loop [16].

## 2. Dissolution/precipitation mechanism

At active oxygen control [10,16–20], the steel is supposed to form magnetite dissociating as:

$$\frac{1}{3}\mathrm{Fe_3O_4(s)} = [\mathrm{Fe}] + \frac{4}{3}[\mathrm{O}] \tag{1}$$

in the hot part of the loop yielding the iron solute concentration (in wppm),

$$\lg(c_{\mathrm{Fe}}) = A_{\mathrm{Fe,s}} + \frac{B_{\mathrm{Fe,s}}}{T} - \frac{4}{3}\lg(c_{\mathrm{O}}) + \frac{4}{3}\left(A_{\mathrm{O,s}} + \frac{B_{\mathrm{O,s}}}{T}\right) - \frac{1}{3\ln 10}(A_{\mathrm{Fe_3O_4}} + B_{\mathrm{Fe_3O_4}}T), \tag{2}$$

---

* Corresponding author. Fax: +49 7247 82 5920/3956.
*E-mail address:* heinrich.muscher@imf.fzk.de (H. Muscher).

0022-3115/$ - see front matter © 2004 Elsevier B.V. All rights reserved.
doi:10.1016/j.jnucmat.2004.07.021

Table 1
Solubility data and Gibbs free energies

| I | $A$ | $B$ | References |
|---|---|---|---|
| Fe, s (wppm) | 6.01 | −4380 (K) | [18,21] |
| O, s (wppm) | 5.2 | −3400 (K) | [18,21] |
| $Fe_3O_4$ | −1110.8 | 0.3245 ($K^{-1}$) | [25] |

where $T$, the absolute temperature (in K), the $A$'s and $B$'s given in Table 1 and applying Henry's law while it precipitates that is reverting reaction (1), at cooler parts.

## 3. Mass transfer model

Applying the one dimensional mass conservation law to the mean concentration, $c$ of non-reacting iron in a volume, $\mathrm{d}V = \pi/4 \cdot d^2 \cdot \mathrm{d}x$ passing streamwise ($x$ direction) with the velocity, $u$ (2 m/s) the surface, $\mathrm{d}A = \pi \cdot d \cdot \mathrm{d}x$ in the duct (of 16 mm hydraulic diameter) during the time, $\partial t$ one finds

$$\left(\frac{\partial}{\partial t}c(t,x) + u\frac{\partial}{\partial x}c(t,x)\right)\mathrm{d}V = j^{\mathrm{w}}(t,x)\mathrm{d}A, \quad (3)$$

where

$$j^{\mathrm{w}}(t,x) = K_{\mathrm{m}}(c^{\mathrm{w}}(t,x) - c(t,x)) \quad (4)$$

is the solute wall flux and

$$K_{\mathrm{m}} = 0.0177u^{0.875}d^{-0.125}\nu^{-0.579}D^{0.704}, \quad (5)$$

an experimentally determined mass transfer coefficient [15] with $D$, the iron diffusion coefficient being typically $10^{-5}$ cm$^2$/s, as explicit given in the key references [21–24] cp [25,26] and $\nu$, the kinematic LBE viscosity, being $1.3 \times 10^{-7}$ m$^2$/s [27–30] at the maximum temperature of 550 °C. The Eq. (5) was primarily derived for constant temperatures. Its applicability to non-isothermal cases (linear temperature gradients in subsequent parts of the loop) is ensured, because *local* mass transfer coefficients are obtained separately for each cell, in which the loop segments are numerically subdivided. This is valid for a large number of quasi-infinitesimal thin volume elements along the loop length. Assuming a fully developed velocity profile of the turbulent flowing LBE ($Re = 2.46 \times 10^6$), Eq. (3) simplifies at steady state to

$$\frac{\mathrm{d}}{\mathrm{d}x}j(x) = K_{\mathrm{m}}\left(c^{\mathrm{w}}(x) - j(x)\frac{4}{\pi d^2 u}\right)\pi d, \quad (6)$$

using the general flux definition,

$$j(x) = \frac{\pi}{4}d^2uc(x). \quad (7)$$

For a closed loop (having the length, $L$ of 35.8 m),

$$\int_0^L j^{\mathrm{w}}(x)\mathrm{d}x = 0 \quad (8)$$

applies while we have at any radial position

$$c(x=0) = c(x=L) \quad (9)$$

so that

$$\int_0^L c(x)\mathrm{d}x = \int_0^L c^{\mathrm{w}}(x)\mathrm{d}x \quad (10)$$

follows, enabling to calculate the mean iron concentration numerically. The wall flux can thus be estimated from Eq. (4) and checked for the requirement (6) until achieving the desired accuracy.

## 4. Results

Fig. 1 shows the temperature profile of the loop and the iron corrosion rate at 0.01 wppm O typical for active oxygen control conditions. Starting at the bottom inlet of the heat exchanger iron dissolves as the temperature increases reaching a maximum of about 180 μm/a at the exit of the second heater where the highest temperature prevails. Keeping that temperature, dissolution declines continuously and finally precipitation starts at the upper inlet of the heat exchanger with its maximum of about 240 μm/a at the bottom exit, assuming that no protective oxide layer limits the corrosion attack. A further temperature decline at the air cooler retards the precipitation. Given the tube thickness of 2.6 mm on average, one may conclude that the loop structure may last for several test campaigns comprising a couple of thousand hours each, provided the model assumptions hold and the fluid properties are correct.

Further, the suggested diffusion coefficient of iron solute in LBE is compared to $4 \times 10^{-5}$ cm$^2$/s provided at 550 °C by the Einstein–Sutherland relation [15,31,32]

$$D = \frac{kT}{4\pi\mu r}, \quad (11)$$

where $k$, the Boltzmann constant (in J K$^{-1}$); $r$, the solute radius, 1.72 Å [33] and $\mu$, the dynamic viscosity, $1.3 \times 10^{-3}$ Pa s [28–30] and to $7.35 \times 10^{-5}$ cm$^2$/s obtained experimentally [34] unfortunately not disclosing any details. That comparison at the dissolution maximum yields striking differences, Fig. 2. Obviously, more rapid diffusion leads to greater dissolution while dissolving more oxygen reduces that effect considerably almost vanishing at about 0.1 wppm. Probably, oxide scales

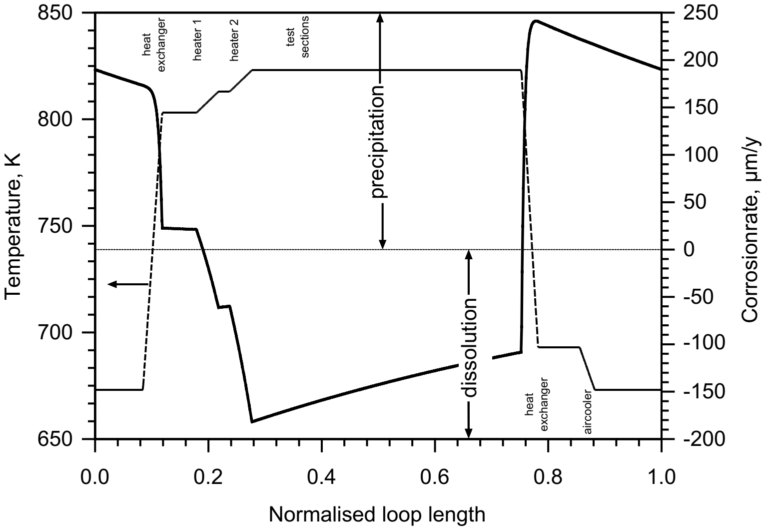

Fig. 1. Temperature profile of the loop and predicted corrosion rate of iron at the wall tubing.

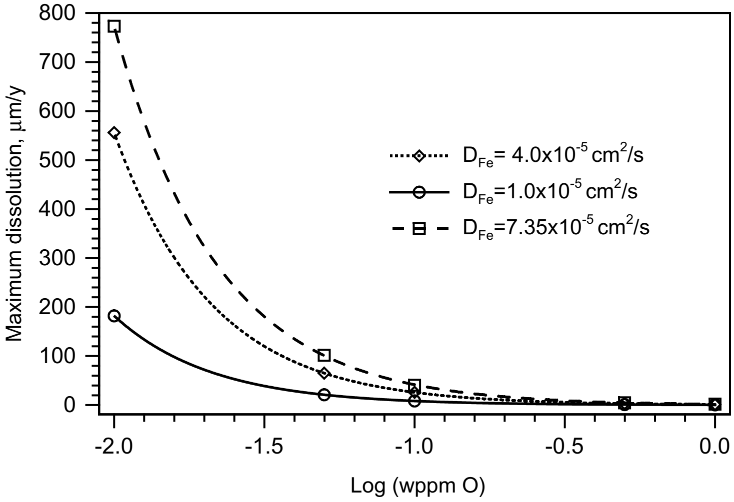

Fig. 2. Effect of the rate of iron diffusion on the maximum dissolution at different wppm O.

form at higher oxygen potentials restricting the iron delivery to the melt/scale interface while also shifting the equilibrium (1) to the left.

## 5. Discussion

The decline in dissolution and precipitation after passing the second heater and on the return flow of the heat exchanger, respectively, may be explained by the downstream effect (DSE) [35–38]. That is, towards progressive saturation the driving force for dissolution/precipitation reduces. Consequently less iron dissolves/precipitates. The maximum dissolution in the vicinity of the test sections may cause some concern with respect to the materials actually tested. The various materials will be located at the duct's centerlines along their lengths (~560 mm). One concern is the iron dissolution stemming from the wall tubing may affect the one expected from the specimens. Probably, the DSE may reduce the extent of dissolution at these sites. Secondly, a streamwise positioning effect may arise. For that, same material will be exposed at the same position in each of the two test sections being about 2.5 m apart.

Above all is the interaction of the dissolved oxygen with the metal solutes especially Fe, Cr and Ni. Indeed, an increased oxygen solubility in liquid Pb in the presence of nickel up to its saturation was found [39,40]. To our knowledge, no such investigations are reported for LBE. Similarly, an influence on the solubility of a particular metal solute in the presence of another may arise. It seems recommendable to study such effects.

Moreover, the influence of the rate of diffusion is of concern since the loop will likely be operated at the lower oxygen levels to allow a considerable safety margin with respect to PbO formation. Whether $7.35 \times 10^{-5}$ $cm^2/s$ reflects a true value or its measurement was contaminated by convective contributions [26,27,41–45] almost unavoidable remains unanswered as details were not reported. Also, $4 \times 10^{-5}$ $cm^2/s$ about four times higher than the suggested value [21] seems not applicable either. Strictly, the relation (11) applies near the melting point [46] which is between 123.5 °C [47,48] and 125 °C [30] for LBE. Certainly, more reliable solute diffusion data are needed to enable proper judgment.

However, extrapolating short term (<5000 h) corrosion data of Cr–Ni steels may provide an indication for the corrosion rate. For example, a weight loss of 124 $\mu g/mm^2$ corresponding to 31 μm/a is reported for AISI 316L after 4500 h at 400 °C, $3.1 \times 10^{-6}$–$7.3 \times 10^{-4}$ wppm O and 3 m/s flow [49] whereas the maximum loop temperature was 550 °C. Further, a rate of 900 μm/a at 500 and 350 °C maximum and minimum temperature, respectively, is reported for such a steel after 1500 h in deoxidized (with 0.05 wt% Mg addition) LBE flowing with up to 1.5 cm/s [9]. At 600 °C maximum temperature and the same temperature difference, a rate of 9 mm/a is estimated [9]. Moreover, 0.1 mm maximum corrosion depth corresponding to 292 μm/a is estimated for such a steel after 3000 h at 450 °C maximum and 400 °C minimum temperature, respectively in saturated oxygen (3.2 wppm) and 1 m/s flow [11]. Apparently, the predicted maximum dissolution of 180 μm/a is a reasonable estimate for the parameters used. Nevertheless, a verification of the model will be performed by using experimental mass transfer data of the test campaigns of martensitic and austenitic steels in the CORRIDA loop of FZK's KALLA lab.

## 6. Conclusions

The model used to analyze the site and extent of corrosion proved very useful in identifying the maximum dissolution predicted at the second heater exit and maximum precipitation at the heat exchanger bottom outlet. Although, the predicted values seem reasonable compared to the few reported experimentally depend strongly on diffusion data requiring the latter to be measured precisely and verifiable. A comparison with experimental loop data can be used to validate the model and increase the accuracy. The tendency of a corrosion increase with an oxygen decrease is understood on the account that more solute is released as the oxide scale grows thinner so that active oxygen control can effectively contribute to lower dissolution.

## Acknowledgment

This work was performed in the framework of the Nuclear Safety Programme of the Forschungszentrum Karlsruhe.

## References

[1] M. Salvatores, Prog. Nucl. Energy 40 (3–4) (2002) 375.

[2] IAEA, Vienna, Technical Meeting to Review of National Programmes on Fast Reactors and Accelerator Systems (ADS), 22–26 April 2002, Karlsruhe.

[3] W.S. Park, T.Y. Song, B.O. Lee, C.K. Park, Nucl. Eng. Des. 219 (2002) 207.

[4] Y. Kurata, M. Futakawa, K. Kikuchi, S. Saito, T. Osugi, J. Nucl. Mater. 301 (2002) 28.

[5] H. Nifenecker, S. David, J.M. Loiseaux, O. Meplan, Nucl. Instrum. and Meth. A 463 (2001) 428.

[6] J.-P. Revol, Prog. Nucl. Energy 38 (2001) 153.

[7] J.J. Park, D.P. Butt, C.A. Beard, Nucl. Eng. Des. 196 (2000) 315.

[8] G. Müller, A. Heinzel, J. Konys, G. Schumacher, A. Weisenburger, F. Zimmermann, V. Engelko, A. Rusanov, V. Markov, J. Nucl. Mater. 301 (2002) 40.

[9] G. Ilinčev, Nucl. Eng. Des. 217 (2002) 167.

[10] J. Knebel, X. Cheng, C. Lefhalm, G. Müller, G. Schumacher, J. Konys, H. Glasbrenner, Nucl. Eng. Des. 202 (2000) 279.

[11] K. Kikuchi, Y. Kurata, S. Saito, M. Futakawa, T. Sasa, H. Oigawa, E. Wakai, K. Miura, J. Nucl. Mater. 318 (2003) 348.

[12] G. Benamati, C. Fazio, H. Piankova, A. Rusanov, J. Nucl. Mater. 301 (2002) 23.

[13] G. Benamati, P. Buttol, C. Fazio, V. Imbeni, C. Martini, G. Palombarini, A. Rusanov, Behaviour of different steels in liquid Pb and Pb–Bi eutectic alloy, Forschungszentrum Karlsruhe GmbH, Karlsruhe, 1999, p. 93.

[14] C. Fazio, I. Ricapito, G. Scaddozzo, G. Benamati, J. Nucl. Mater. 318 (2002) 325.

[15] F. Balbaud-Célérier, F. Barbier, J. Nucl. Mater. 289 (2001) 227.

[16] J.U. Knebel, X. Cheng, G. Müller, G. Schumacher, J. Konys, O. Wedemeyer, G. Grötzbach, L. Carteciano, Thermohydraulic and materials specific investigations into the realization of an accelerator driven system (ADS) to transmute minor actinides 1999 status report, Wissenschaftliche Berichte FZKA 6506, Forschungszentrum Karlsruhe GmbH, Karlsruhe, 2000.

[17] J.U. Knebel, G. Müller, J. Konys, Lead–bismuth activities at the Karlsruhe lead laboratory Kalla, in: Proceedings of the 10th International Conference on Nuclear Engineering (ICONE10), 14–18 April 2002, Arlington, VA, ASME, New York, NY, 2002, ICONE10-22240.

[18] N. Li, J. Nucl. Mater. 300 (2002) 73.

[19] H. Muscher, Measurement of oxygen activities in eutectic lead–bismuth by means of the EMF method Wissenschaftliche Berichte FZKA-6690, Forschungszentrum Karlsruhe GmbH, Karlsruhe, 2001.

[20] J. Konys, H. Muscher, Z. Voss, O. Wedemeyer, J. Nucl. Mater. 296 (2001) 289.

[21] B.X. He, N. Li, M. Mineev, J. Nucl. Mater. 297 (2001) 214.

[22] J. Sannier, G. Santarini, J. Nucl. Mater. 107 (1982) 196.

[23] J. Zhang, N. Li, J. Nucl. Mater. 321 (2003) 184.

[24] J. Zhang, N. Li, Nucl. Technol. 144 (2003) 379.

[25] I. Barin, Thermochemical Data of Pure Substances, VCH, Weinheim, 1989.

[26] V. Botton, P. Lehmann, R. Bolcato, R. Moreau, R. Haettel, Int. J. Heat Mass Transfer 44 (2001) 3345.

[27] V. Botton, P. Lehmann, R. Bolcato, R. Moreau, Energ. Convers. Manage. 43 (2002) 409.

[28] C.B. Davis, A.S. Shieh, Overview of the use of Athena for thermal-hydraulic analysis of systems with lead–bismuth coolant, in: Proceedings of the 8th International Conference on Nuclear Engineering (ICONE8), 2–6 April 2000, Baltimore, MD, ASME, New York, NY, 2000.

[29] F. Venneri, M. Williamson, N. Li, M. Houts, R. Morley, D. Beller, W. Sailor, G. Lawrence, Disposition of nuclear wastes using subcritical accelerator-driven systems, in: Proceedings of the Uranium Institute 24th Annual International Symposium, 9–10 September 1999, London, Uranium Institute, London, 1999.

[30] J.K. Fink, Pb–Bi eutectic viscosity preliminary recommendation, available at http://www.insc.anl.gov/matprop/pbbi/pbbiviscosity.pdf.

[31] H.U. Borgstedt, C. Guminski, J. Nucl. Mater. 303 (2002) 240.

[32] A.S. Chauhan, R. Ravi, R.P. Chhabra, Chem. Phys. 252 (2000) 227.

[33] R.C. Weast, M.J. Astle, W.H. Beyer (Eds.), CRC Handbook of Chemistry and Physics, 67th Ed., CRC, Boca Raton, FL, 1987.

[34] R.I. Hodge, R.B. Turner, J.L. Platten, 5000-hr test of a eutectic Pb–Bi circuit constructed in steel and niobium, in: J.E. Draley, J.R. Weeks (Eds.), Corrosion by Liquid Metals, Plenum, New York, NY, 1970, p. 283.

[35] H.U. Borgstedt, J. Nucl. Mater. 317 (2003) 160.

[36] T. Suzuki, T. Mutoh, J. Nucl. Mater. 140 (1) (1986) 56.

[37] S. Casadio, A. Saltelli, J. Nucl. Mater. 87 (1) (1979) 203.

[38] M.V. Polley, G. Skyrme, J. Nucl. Mater. 66 (3) (1977) 221.

[39] A. Taskinen, Acta Polytech. Scand. Chem. Incl. Metall. Ser. 146 (1981) 1.

[40] A. Taskinen, Scand. J. Metall. 10 (4) (1981) 184.

[41] R.W. Smith, X. Zhu, M.C. Tunniclié, T.J.N. Smith, L. Misener, J. Adamson, Ann. NY Acad. Sci. 974 (2002) 57.

[42] D.J. Maclean, T. Alboussiére, Int. J. Heat Mass Transfer 44 (2001) 1639.

[43] T. Itami, T. Masaki, H. Aoki, S. Munejiri, M. Uchida, S. Matsumoto, K. Kamiyama, K. Hoshino, J. Non-Cryst. Solids 312–314 (2002) 177.

[44] C. Barat, J.P. Garandet, Int. J. Heat Mass Transfer 39 (10) (1996) 2177.

[45] G. Mathiak, A. Griesche, K.H. Kraatz, G. Frohberg, J. Non-Cryst. Solids 205–207 (1996) 412.

[46] V.N. Eremenko, Y.V. Natanzon, Transl. Dokl. Akad. Nauk SSSR 291 (5) (1986) 1147.

[47] B.F. Gromov, Y.I. Orlov, P.N. Martynov, K.D. Ivanov, V.A. Gulevsky, Physico-chemical properties of lead–bismuth coolant technology, in: H.U. Borgstedt, G. Frees, (Eds.), Proceedings of the International Seminar Liquid Metal Systems 2, 16–18 March 1993, Karlsruhe, 1995, p. 339.

[48] B.F. Gromov, J.I. Orlov, V.A. Gulevsky, Physico-chemical properties of Pb–Bi eutectic used as coolant for liquid metal target, in: H. Condé (Ed.), Proceedings of the 2nd International Conference ADTTA, 3–7 June 1996, Kalmar, vol. 2, Uppsala University, Kalmar, 1997, p. 912.

[49] B. Long, G. Scaddozzo, C. Fazio, M. Agostini, A. Aiello, G. Benamati, Corrosion behaviour of steels and refractory metals in flowing Pb–Bi, Interim report, 2003.